A Microenvironment-Sensitive Fluorescent Pyrimidine Ribonucleoside Analogue: Synthesis, Enzymatic Incorporation, and Fluorescence Detection of a DNA Abasic Site

ARTICLE *in* CHEMISTRY - A EUROPEAN JOURNAL · NOVEMBER 2011

Impact Factor: 5.73 · DOI: 10.1002/chem.201101194 · Source: PubMed

2 AUTHORS:

Arun Tanpure
Indian Institute of Science Education and R…
10 PUBLICATIONS **116** CITATIONS
SEE PROFILE

Seergazhi G Srivatsan
Indian Institute of Science Education and R…
30 PUBLICATIONS **756** CITATIONS
SEE PROFILE

CHEMISTRY
A EUROPEAN JOURNAL

DOI: 10.1002/chem.201101194

A Microenvironment-Sensitive Fluorescent Pyrimidine Ribonucleoside Analogue: Synthesis, Enzymatic Incorporation, and Fluorescence Detection of a DNA Abasic Site

Arun A. Tanpure and Seergazhi G. Srivatsan*[a]

Abstract: Base-modified fluorescent ribonucleoside-analogue probes are valuable tools in monitoring RNA structure and function because they closely resemble the structure of natural nucleobases. Especially, 2-aminopurine, a highly environment-sensitive adenosine analogue, is the most extensively utilized fluorescent nucleoside analogue. However, only a few isosteric pyrimidine ribonucleoside analogues that are suitable for probing the structure and recognition properties of RNA molecules are available. Herein, we describe the synthesis and photophysical characterization of a small series of base-modified pyrimidine ribonucleoside analogues derived from tagging indole, *N*-methylindole, and benzofuran onto the 5-position of uracil. One of the analogues, based on a 5-(benzofuran-2-yl)pyrimidine core, shows emission in the visible region with a reasonable quantum yield and, importantly, displays excellent solvatochromism. The corresponding triphosphate substrate is effectively incorporated into oligoribonucleotides by T7 RNA polymerase to produce fluorescent oligoribonucleotide constructs. Steady-state and time-resolved spectroscopic studies with fluorescent oligoribonucleotide constructs demonstrate that the fluorescent ribonucleoside photophysically responds to subtle changes in its environment brought about by the interaction of the chromophore with neighboring bases. In particular, the emissive ribonucleoside, if incorporated into an oligoribonucleotide, positively reports the presence of a DNA abasic site with an appreciable enhancement in fluorescence intensity. The straightforward synthesis, amicability to enzymatic incorporation, and sensitivity to changes in the microenvironment highlight the potential of the benzofuran-conjugated pyrimidine ribonucleoside as an efficient fluorescent probe to investigate nucleic acid structure, dynamics, and recognition events.

Keywords: abasic sites · DNA · fluorescent probes · ribonucleosides · RNA

Introduction

Fluorescent nucleoside analogues that photophysically report changes in nucleic acid conformation have become very important bioanalytical tools in advancing the understanding of nucleic acid structure and function.[1–7] Nucleic acids lack intrinsic fluorescence as natural nucleobases are practically nonemissive.[8] In order to impart better photophysical properties to otherwise nonemissive natural nucleobases, most design principles rely on utilizing naturally occurring fluorescent heterocycles or polycyclic aromatic hydrocarbons or on extending the π conjugation by appending heterocycles to the bases.[6] By utilizing these design strategies, several classes of base-modified fluorescent nucleobase analogues, size-expanded,[9] extended,[6,10] pteridine,[11] polycyclic aromatic hydrocarbon,[9] and isomorphic,[6] have been developed. A significant number of these analogues that display useful photophysical properties have been implemented in DNA-based and, to a relatively lesser extent, in RNA-based biophysical assays.[12,13] Notably, the majority of these analogues, except isomorphic bases, substantially deviate from the native structure of the nucleobases. Isomorphic analogues are advantageous because they maintain the Watson–Crick (WC) base pairing and minimally perturb the native structure and function of target oligonucleotides. In particular, a highly emissive and environment-sensitive adenosine analogue, 2-aminopurine (2AP), has been extensively utilized in designing several DNA- and RNA-based biophysical and discovery assays.[7,14,15] However, excitation and emission maxima in the UV region and the drastically low quantum yields displayed by 2AP when incorporated into oligonucleotides greatly limit its application to in vitro systems only.[15,16]

Numerous base-modified ribonucleoside analogues with emission in the visible region and a high quantum yield have been developed, but only a few analogues have been effectively implemented in exploring the functions of RNA

[a] A. A. Tanpure, Dr. S. G. Srivatsan
Department of Chemistry
Indian Institute of Science Education and Research
Sai Trinity Building, Pashan, Pune 411021 (India)
Fax: (+91) 20-25899790
E-mail: srivatsan@iiserpune.ac.in

Supporting information for this article is available on the WWW under http://dx.doi.org/10.1002/chem.201101194. It contains details of the synthesis of the modified ribonucleosides, photophysical characterizations of the ribonucleoside analogues and RNA transcripts, MALDI-TOF MS analyses of the RNA transcripts, quenching studies, thermal denaturation studies, gel mobility shift experiments, and NMR and mass spectra of the compounds.

molecules.[7] In particular, only a very few structurally nonperturbing pyrimidine ribonucleoside analogues have shown promise as useful fluorescent probes.[17–19] In order to expand the repertoire of useful fluorescent pyrimidine ribonucleoside analogues, we sought to synthesize microenvironment-sensitive pyrimidine ribonucleoside analogues that are structurally nonperturbing, display emission in the visible region, and maintain a reasonable quantum yield upon incorporation into oligoribonucleotides.

We have drawn inspiration from a naturally occurring fluorescent amino acid, tryptophan, to construct a series of emissive pyrimidine ribonucleoside analogues. Tryptophan, an indole derivative, is reasonably emissive, and its emission properties are highly sensitive to its local environment.[20] Therefore, we hypothesize that the attachment of a bicyclic heterocycle such as an indole moiety to a nucleobase (for example, to the 5-position of uracil) may enhance the π conjugation and impart better photophysical properties to the nucleobase.[21,22] Herein, we describe the synthesis and photophysical characterization of a focused set of new pyrimidine ribonucleoside analogues derived by tagging indole, *N*-methylindole, and benzofuran at the 5-position of uracil. Notably, the benzofuran-conjugated uridine analogue is appreciably emissive, with an emission maximum in the visible region, and it also exhibits excellent solvatochromism. We also report the synthesis of the corresponding ribonucleoside triphosphate substrate and its effective incorporation into RNA oligonucleotides by transcription reactions catalyzed by T7 RNA polymerase. Furthermore, the emissive uridine analogue, when incorporated into an oligoribonucleotide, positively signals the presence of a DNA abasic site.

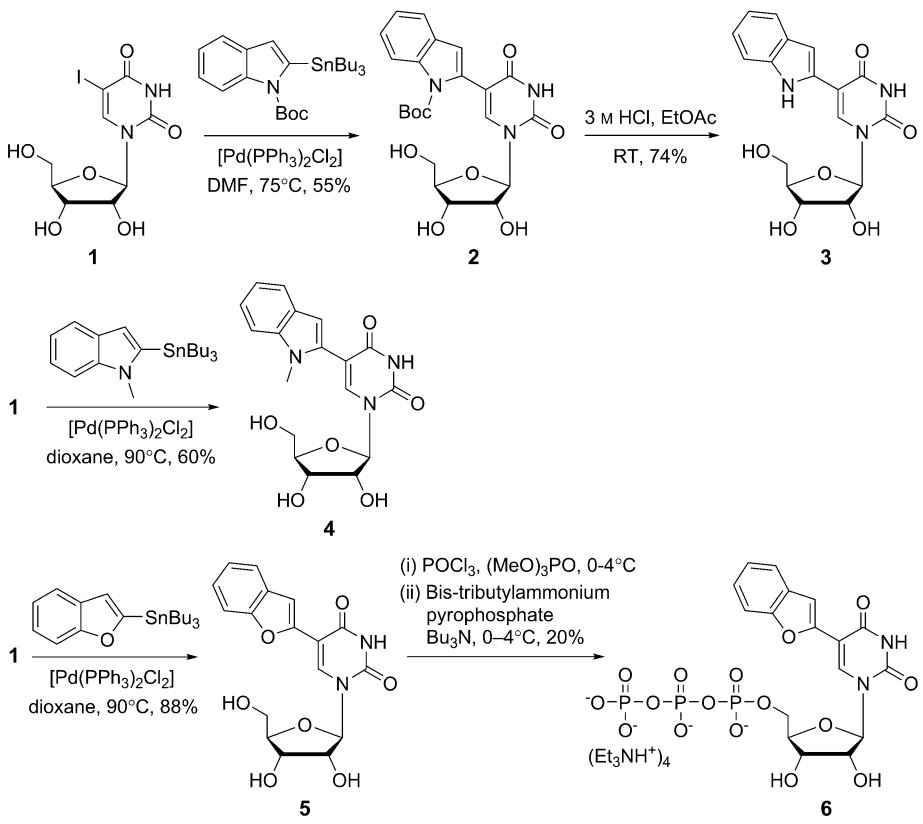

Scheme 1. Synthesis of modified ribonucleoside analogues **3**–**5** and ribonucleotide analogue **6**. See the Supporting Information for experimental details. Boc: tert-butoxycarbonyl; DMF: *N*,*N*-dimethylformamide.

Results and Discussion

Synthesis of ribonucleoside analogues: Modified uridine analogues **3**–**5** have been synthesized according to the procedure illustrated in Scheme 1. In a two-step reaction, indole-conjugated uridine **3** has been synthesized by performing a palladium-catalyzed cross-coupling reaction between 5-iodouridine (**1**) and a tributylstannyl derivative of *N*-Boc-protected indole, followed by removal of the Boc group in the presence of 3 M HCl. The *N*-methylindole- and benzofuran-conjugated uridines, **4** and **5**, have been synthesized by treating 5-iodouridine (**1**) with the corresponding stannylated heterocycles in the presence of a palladium catalyst.

Photophysical characterization of ribonucleoside analogues: An important attribute exhibited by many conformation-sensitive fluorescent nucleoside-analogue probes is that they photophysically respond to changes in solvent polarity.[6] Therefore, prior to incorporation into RNA oligonucleotides, the photophysical properties have been examined in solvents of different polarity to evaluate the responsiveness of the modified ribonucleosides to polarity changes. An increase in solvent polarity has marginal impact on the ground-state electronic spectrum of modified ribonucleosides **3**–**5** (Figure 1 and Table 1).[23] However, the quantum yield, emission maximum, and fluorescence lifetime are significantly affected by the solvent polarity. Unexpectedly, the indole- and *N*-methylindole-conjugated uridine analogues (**3** and **4**, respectively) show very weak fluorescence in nonpolar solvents and practically no fluorescence in water (Figures S1 and S2 and Table S1 in the Supporting Information). Rewardingly, if excited at its lowest energy maximum (322 nm), the benzofuran-conjugated uridine **5** in water exhibits a very strong emission band ($\lambda_{em}=447$ nm) that corresponds to a quantum yield of 0.212 ± 0.002 (Figure 1,

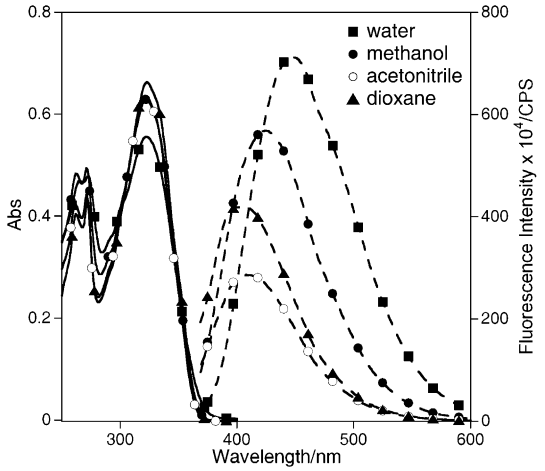

Figure 1. Absorption (25 μM, solid lines) and emission (5.0 μM, dashed lines) spectra of ribonucleoside **5** in various solvents. Samples were excited at 322 nm. Excitation and emission slit widths were maintained at 2 and 4 nm, respectively. All solutions for absorption and emission studies contained 2.5% and 0.5% dimethylsulfoxide (DMSO), respectively.

Table 1. Photophysical properties of fluorescent ribonucleoside analogue **5** in various solvents.[25]

Solvent	λ_{max}[a] [nm]	λ_{em} [nm]	I_{rel}[b]	Φ[c]	τ_{av}[c] [ns]	k_r/k_{nr}[d]
water	322	447	1.0	0.212	2.55	0.27
methanol	322	423	0.8	0.145	0.94	0.16
acetonitrile	322	410	0.4	0.063	0.33	0.06
dioxane	322	404	0.6	0.099	0.43	0.11

[a] The lowest energy maximum is given. [b] Emission intensity relative to intensity in water. [c] Standard deviations for the quantum yield (Φ) and average lifetime (τ_{av}) are $\leq$0.004 and 0.02 ns, respectively. [d] k_r and k_{nr} are radiative and nonradiative decay rate constants, respectively.

Table 1). As the solvent polarity is sequentially decreased from water to dioxane, the ribonucleoside shows a significant hypsochromic shift (447 to 404 nm) and a nearly twofold quenching in fluorescence intensity. Furthermore, the relative quantum yield determined by using 2AP as a standard in various solvents is in good agreement with the observed fluorescence intensity in the respective solvents (Table 1). The responsiveness of the ribonucleoside to changes in the solvent-polarity environment is also confirmed by plotting the Stokes shift in various solvents as a function of Reichardts' microscopic solvent polarity parameter, $E_T(30)$ (Figure S3 in the Supporting Information).[24] A positive correlation between the Stokes shift and $E_T(30)$ further establishes the sensitiveness of the emissive ribonucleoside **5** to its surrounding environment.

Time-resolved fluorescence spectroscopic measurements have also been performed to study the effect of solvent polarity on the excited-state decay kinetics of ribonucleoside **5** (Table 1, Figure S4 in the Supporting Information). The decay profile of the emissive ribonucleoside in solvents of different polarity reveals distinct decay kinetics. The ribonucleoside in water has the highest lifetime of 2.55 ns. As the polarity decreases when the solvent is changed from water to dioxane, a huge decrease in the lifetime (approximately sixfold) is observed in dioxane relative to that in water. The decreasing trend in the lifetime is consistent with the intensity displayed by the ribonucleoside in various solvents. Radiative (k_r) and nonradiative (k_{nr}) decay rate constants in different solvents have been calculated by using experimentally determined lifetimes and quantum yields (Table 1). A nearly 2.5-fold higher k_r/k_{nr} ratio in water clearly indicates that the radiative pathway is appreciably favored in water relative to that in dioxane. Properties such as emission in the visible region, a modest quantum yield, and responsiveness to polarity changes as illustrated by fluorescence measurements adequately confer probelike attributes to the fluorescent ribonucleoside analogue **5**. Therefore, ribonucleoside **5** has been selected for incorporation into RNA oligonucleotides by transcription reactions. The corresponding ribonucleoside triphosphate substrate **6**, which is necessary for in vitro transcription reactions, has been synthesized by employing the method developed by Ludwig.[26] The modified triphosphate **6** has been synthesized in a one-pot two-step reaction by treating ribonucleoside **5** with freshly distilled $POCl_3$, followed by a reaction with bistributylammonium pyrophosphate (Scheme 1).

Enzymatic incorporation: Although, solid-phase chemical synthesis is the method of choice for the synthesis of modified oligoribonucleotides, enzymatic methods such as transcription and ligation reactions have also been effectively utilized in labeling RNAs.[27–29] In order to investigate the ability of T7 RNA polymerase to incorporate the modified triphosphate **6** into oligoribonucleotides, in vitro transcription reactions were conceived, as illustrated in Figure 2. A series of promoter–template duplexes were assembled by annealing a DNA promoter strand to DNA templates, **D1**–**D5** (Figure 2). The templates were designed to contain one or two deoxyadenosine residues at different positions to direct single or double incorporations of the modified triphosphate **6**. Additionally, a deoxythymidine residue was placed at the 5′-end of each template strand to direct the addition of a single adenosine at the 3′-end of each transcript. Hence, in vitro transcription reactions in the presence of GTP, CTP, UTP/**6**, and α-^{32}P ATP, if successful, would result in the formation of full-length oligoribonucleotide transcripts containing a ^{32}P-labeled adenosine at the 3′-end. Reaction products could then be resolved by analytical denaturing polyacrylamide gel electrophoresis and imaged. Failed transcription reactions that resulted in transcripts shorter than the full-length products would not carry the ^{32}P-labeled adenosine and, hence, would remain undetected.

A transcription reaction in the presence of template **D1** results in the formation of the 10-mer modified full-length RNA transcript **8** containing the modified ribonucleoside at the +7 position (Figure 3, lane 2). Along with the full-length product, trace amounts of $N+1$ and $N+2$ products are also formed due to nontemplated random incorporation of ribonucleotides.[30] The triphosphate **6** is incorporated into the oligoribonucleotide with a moderate efficiency of

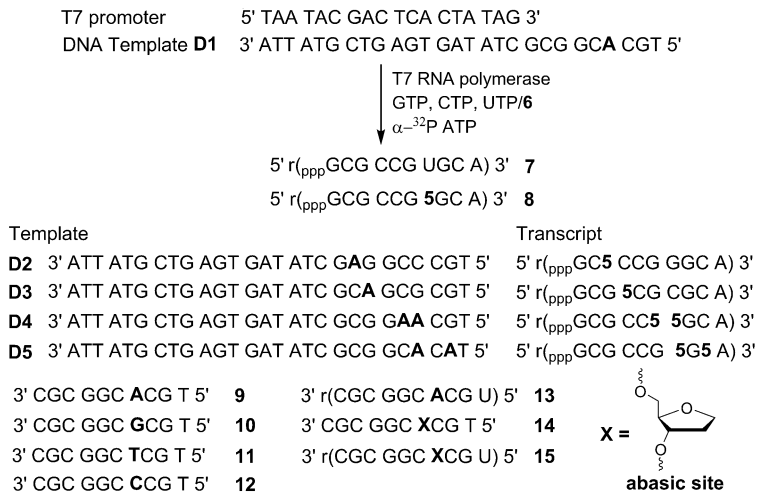

Figure 2. Top: Incorporation of ribonucleoside triphosphate **6** by transcription reactions in the presence of DNA templates **D1**–**D5**. Bottom: Sequences of the synthetic oligonucleotides (**9**–**15**) used in this study. "r" preceding the parentheses with the sequence indicates an RNA oligonucleotide. See the Experimental Section for details.

(67±3)% relative to the reaction in the presence of natural UTP. Discernible retardation in the mobility of modified transcript **8** with respect to unmodified transcript **7** clearly indicates the inclusion of the higher molecular weight emissive ribonucleoside during the transcription reaction (Figure 3, compare lanes 1 and 2). When neither UTP nor **6** is included in a control transcription reaction, the full-length RNA product is not produced (Figure 3, lane 3). This result shows that the formation of full-length transcripts is not due to adventitious misincorporation. Interestingly, in a reaction containing UTP and **6** in equimolar concentrations, T7 RNA polymerase incorporates both the natural and the modified UTP into RNA transcripts (Figure 3, lane 4).

In order to test the ability of T7 RNA polymerase to incorporate the modification near the promoter region, transcription reactions were performed with templates **D2** and **D3**, which would direct the incorporation of **6** at the +3 and +4 positions, respectively.[31] The incorporation efficiencies were found to be lower for reactions with templates **D2** and **D3** (Figure 3, lanes 6 and 8). Notably, reactions in the presence of templates **D4** and **D5** resulted in double incorporation of **6** in successive as well as separate sites (Figure 3, lanes 10 and 12). Albeit with moderate yields, the reactions with various templates clearly demonstrate the usefulness of in vitro transcription reactions in generating singly and doubly modified fluorescent oligoribonucleotides.

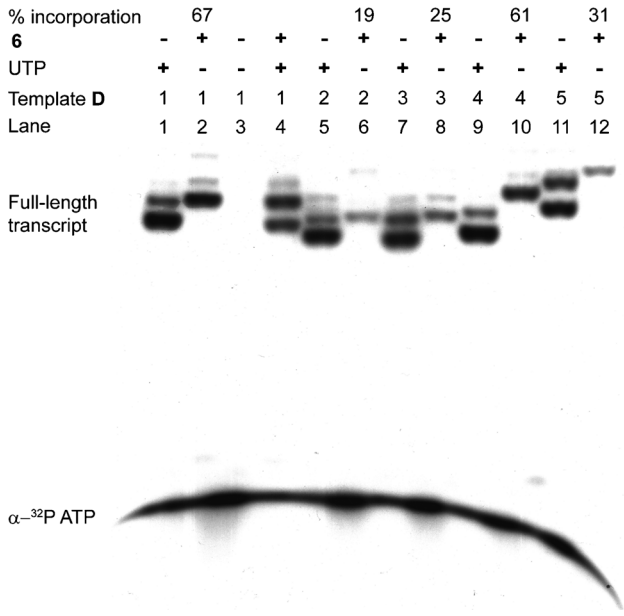

Figure 3. Polyacrylamide gel electrophoresis of transcripts obtained from in vitro transcription reactions with DNA templates **D1**–**D5** in the presence of UTP and modified UTP **6** under denaturing conditions. The percentage incorporation of **6** is reported with respect to the amount of full-length product formed in the presence of UTP. All reactions were performed in duplicate and the errors in yields were ≤4%. See the Experimental Section for details.

Characterization of fluorescent oligoribonucleotide transcripts: Large-scale transcription reactions were performed in the presence of non-radiolabeled triphosphates and template **D1** to isolate transcript **8** for further chemical and photophysical characterizations (Figure S5 in the Supporting Information). A typical reaction after gel electrophoretic purification gave nearly 14 nmol of the modified oligoribonucleotide product. The presence of benzofuran-conjugated uridine **5** in oligoribonucleotide **8** was confirmed by MALDI-TOF mass analysis (Figure 4). Furthermore, reversed-phase HPLC analysis of ribonucleoside products obtained from an enzymatic digestion reaction of transcript **8** clearly revealed the presence of modified ribonucleoside **5** (Figure 5). The ribonucleoside composition determined from the area under the individual ribonucleoside peak also matched well with the sequence of the full-length oligoribonucleotide. Mass analysis of HPLC fractions corresponding to the retention time of each ribonucleoside unambiguously established the authenticity of the modified ribonucleoside present in transcript **8** (Table S2 in the Supporting Information).[25] Together, these results clearly reveal the incorporation of the emissive ribonucleotide into RNA oligonucleotides by RNA polymerase in transcription reactions.

Photophysical characterization of fluorescent oligoribonucleotides: The fluorescence properties of emissive nucleo-

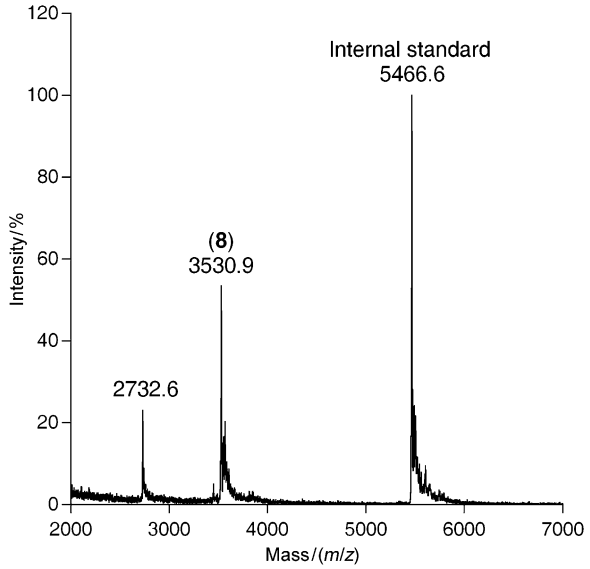

Figure 4. MALDI-TOF MS spectrum of modified transcript **8** calibrated relative to the +1 ion of an internal 18-mer DNA oligonucleotide standard (m/z 5466.6). m/z 2732.6 is the +2 ion of the internal DNA standard. m/z calcd for **8**: 3531.0 [M]; found: 3530.9.

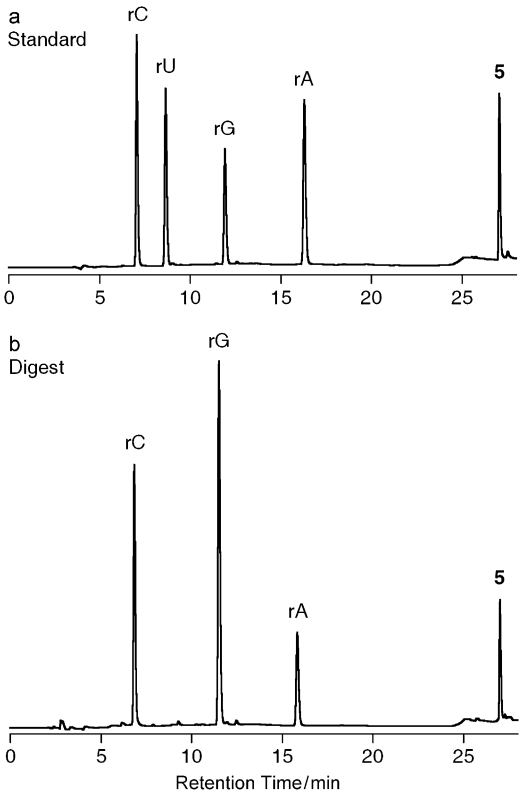

Figure 5. HPLC profile of ribonucleoside products obtained from an enzymatic digestion of transcript **8** at $\lambda = 260$ nm. a) Mixture of natural ribonucleosides and modified fluorescent ribonucleoside **5**; b) digested oligoribonucleotide **8**. See the Experimental Section for details.

side analogues incorporated into oligonucleotides are known to be influenced by a variety of mechanisms involving neighboring bases.[15,21,32,33] Therefore, steady-state and time-resolved fluorescence spectroscopic measurements have been carried out with oligoribonucleotide **8** and duplexes of **8** to evaluate the influence of neighboring bases on the fluorescence of ribonucleoside **5**. A series of duplexes have been assembled by hybridizing oligoribonucleotide **8** to complementary DNA and RNA oligonucleotides, in which the ribonucleoside **5** has been placed opposite complementary or mismatched bases (Figure 2).

The photophysical properties of oligoribonucleotide **8** reveal characteristic features that are different from those of the free ribonucleoside **5** in aqueous buffer. Upon excitation, the single-stranded oligoribonucleotide **8** shows an emission band centered around 447 nm and corresponding to a quantum yield of 0.040 ± 0.001, which is nearly fivefold lower than that of the free ribonucleoside (Figure 6, Table S3 in the Supporting Information). Unlike the free ribonucleoside, which exhibits monoexponential fluorescence-intensity decay kinetics, oligoribonucleotide **8** displays biexponential decay kinetics (Figure S6 and Table S3 in the Supporting Information). The biexponential decay kinetics consists of a shorter and a longer lifetime component, both of which contribute equally to the overall lifetime ($\tau_{av} =$ 2.21 ns). Similar decay profiles have been reported for 2AP, in that the free nucleoside exhibits decay kinetics corresponding to a single lifetime, but if the nucleoside is incorporated into an oligonucleotide, it shows decay kinetics corresponding to multiple lifetimes.[34] The quenching of ribonucleoside fluorescence in **8** may possibly be due to an electron-transfer process between the modified base and neighboring bases or to alterations in the conformation of the benzofuran moiety with respect to the nucleobase.[21,33–35] Several emissive nucleoside analogues containing conjugated and fused heterocycles, if incorporated into oligonucleotides, show similar fluorescence quenching.[6]

The fluorescence quenching is much more pronounced in RNA–DNA (**8·9**) and RNA–RNA (**8·13**) duplexes in which the emissive ribonucleoside **5** is placed opposite to the complementary bases, dA and A, respectively (Figure 6). Du-

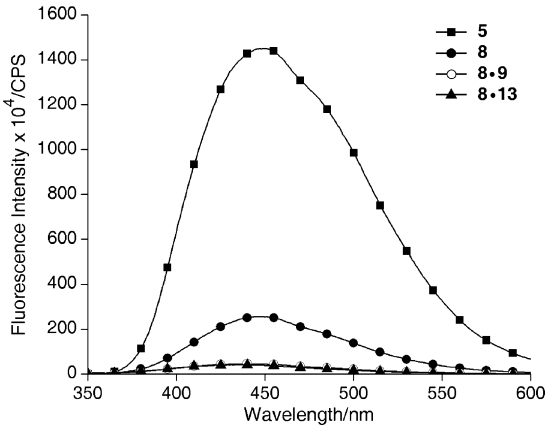

Figure 6. Emission spectra (measured at 1 μM) of ribonucleoside **5**, single-stranded RNA transcript **8**, and duplexes **8·9** and **8·13** in cacodylate buffer (20 mM, pH 7.1). Samples were excited at the absorption maximum of the ribonucleoside ($\lambda = 322$ nm) with an excitation slit width of 4 nm and emission slit width of 7 nm.[25]

plexes **8·9** and **8·13** show slightly blueshifted emission maxima (approximately 439 nm), which correspond to quantum yields of $(0.0085 \pm 1.0) \times 10^{-4}$ and $(0.0082 \pm 2.1) \times 10^{-4}$, nearly four- and fivefold lower than that of the single-stranded oligoribonucleotide **8**, respectively (Table S3 in the Supporting Information). The perfect duplexes also show biexponential decay kinetics similar to that of **8** (Figure S8 in the Supporting Information). The drastic quenching of fluorescence intensity accompanied by a small spectral shift in perfect duplexes **8·9** and **8·13** may possibly be due to a combination of the following reasons: a) an electron-transfer process between the base-paired fluorescent analogue and flanking bases, b) a desolvation effect, or c) alterations in the conformation of the labeled uridine.[15,21,33]

Interestingly, mismatched duplexes **8·10**, **8·11**, and **8·12**, which contain **5** opposite to dG, dT, and dC, respectively, exhibit two- to threefold higher fluorescence intensity than the perfect duplexes (Figure S9 in the Supporting Information). Similar to the perfect duplexes, all mismatched duplex constructs display biexponential decay kinetics with varying shorter and longer lifetime components (Figure S10 and Table S3 in the Supporting Information). Collectively, these results demonstrate the ability of ribonucleoside **5** to photophysically distinguish between a single-stranded oligonucleotide and a perfect complementary duplex, albeit with quenched emission. Nevertheless, this trait of ribonucleoside **5** can be utilized in hybridization assays, in that the kinetics of formation and dissociation of a perfect duplex can be studied by monitoring changes in the photophysical properties of the fluorescently modified oligoribonucleotide.[18b,36]

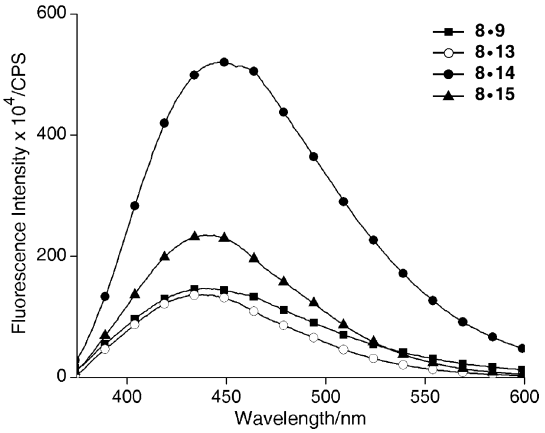

Figure 7. Emission spectra (measured at 1 μM) of duplexes containing the emissive ribonucleoside **5** opposite to complementary bases (**8·9** and **8·13**) and abasic sites (**8·14** and **8·15**) in cacodylate buffer (20 mM, pH 7.1). Samples were excited at 330 nm with an excitation slit width of 7 nm and emission slit width of 9 nm.[25]

Fluorescence detection of a DNA abasic site: Abasic sites are frequently occurring DNA lesions that are vulnerable to strand breaks and, if unrepaired, can be toxic as well as mutagenic.[37,38] Most methods that have been developed to detect abasic sites either use aldehyde-reactive probes, which irreversibly react with abasic sites of isolated DNA, or fluorescent probes, which show changes in fluorescence properties if placed opposite to abasic sites.[12d,39,40] The drastic quenching in fluorescence intensity upon placement of the fluorescent probe **5** opposite to complementary bases prompted us to study the effect of abasic sites on the fluorescence properties of **5**. Abasic-site-containing duplexes have been constructed by hybridizing RNA transcript **8** to custom DNA and RNA oligonucleotides **14** and **15**, which contain a chemically stable abasic-site surrogate, tetrahydrofuran (Figure 2). When excited at 330 nm, the abasic-site-containing duplex **8·14** shows a strong emission band ($\lambda_{em} =$ 447 nm), which corresponds to a quantum yield of $0.034 \pm$ 0.001, nearly fourfold higher than that of the perfect duplex **8·9** (Figure 7, Table S3 in the Supporting Information). Interestingly, RNA–RNA duplex **8·15**, which possesses an abasic site opposite to **5**, exhibits only a slight enhancement in fluorescence intensity relative to that of the equivalent perfect duplex **8·13** (Figure 7, Table S3 in the Supporting Information). The comparable emission maxima of duplex **8·14** and free ribonucleoside **5** in aqueous buffer indicates that the solvent-polarity environment around the fluorophore in **8·14** and the free nucleoside is similar (Table S3 in the Supporting Information). In addition, a fourfold higher k_r/k_{nr} ratio, calculated from the Φ and τ values, indicates that the radiative pathway is appreciably favored in the abasic-site-containing duplex **8·14** over the perfect duplex (Table S3 in the Supporting Information). Therefore, the emissive ribonucleoside, when incorporated into an oligoribonucleotide, preferentially signals the presence of a DNA abasic site with a significant enhancement in fluorescence intensity.

Stability of the duplexes: The modified ribonucleoside upon incorporation can potentially perturb the native structure of oligoribonucleotides, which can lead to ineffective hybridization. The observed fluorescence properties of the duplexes would then be a consequence of a mixture of the more emissive single-stranded oligoribonucleotide **8** and the corresponding duplex. In order to investigate the influence of benzofuran modification on the duplex stablity, thermal denaturation and radioactive native gel mobility shift experiments were performed under the conditions employed in the fluorescence experiments. Slightly lower T_m values for the modified duplexes relative to those of the corresponding control unmodified duplexes indicated a marginal destabilization due to benzofuran modification (Figure S11 and S12 and Table S4 in the Supporting Information). ^{32}P-labeled transcript **8**, synthesized by a transcription reaction in the presence of template **D1** and α-^{32}P ATP, was annealed to custom oligonucleotides **9**–**15**. The hybridized oligonucleotides were resolved on a nondenaturing polyacrylamide gel and imaged. The gel shift experiments revealed complete hybridization (Figure 8). Taken together, these results clearly indicate that the benzofuran moiety does not affect the hybridization efficiency. Hence, it can be concluded that the observed differences in the fluorescence properties of completely intact duplexes are exclusively due to differences in the microenvironment of the fluorescent ribonucleoside.

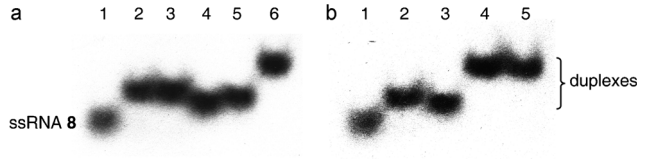

Figure 8. Gel mobility shift experiments to determine the hybridization efficiency of duplexes containing the emissive ribonucleoside **5** opposite to complementary bases, mismatched bases, and abasic sites. a) Lane 1: single-stranded oligoribonucleotide **8**; lanes 2–6: duplexes **8·9**, **8·11**, **8·10**, **8·12**, and **8·13**, respectively. b) Lane 1: oligoribonucleotide **8**; lanes 2–5: duplexes **8·9**, **8·14**, **8·13**, and **8·15**, respectively.

Conclusion

Incorporation of the modified ribonucleoside reporter near the interaction site and close maintainance of the structural and functional integrity of the target oligoribonucleotide will provide a better understanding of the interaction under investigation. In this regard, microenvironment-sensitive emissive pyrimidine ribonucleoside analogue **5**, which is minimally perturbing and displays emission in the visible region with a reasonable quantum yield, has the potential to be implemented in fluorescence-based assays to investigate nucleic acid structure, dynamics, and recognition processes. Efforts to explore therapeutically relevant RNA–protein and RNA–small-molecule interactions by using the labeled oligoribonucleotides are currently in progress.

Experimental Section

Enzymatic incorporation of ribonucleoside triphosphate 6:

Transcription reactions with α-^{32}P ATP: Promoter–template duplexes were assembled by heating a 1:1 mixture (final concentration: 5 μM) of the deoxyoligonucleotide template (**D1**–**D5**) and an 18-mer T7 RNA polymerase consensus promoter deoxyoligonucleotide sequence in TE buffer (10 mM tris(hydroxymethyl)aminomethane/HCl (Tris-HCl), 1 mM ethylenediaminetetraacetate (EDTA), 100 mM NaCl, pH 7.8) at 90 °C for 3 min and cooling the solution slowly to room temperature. The duplexes were then placed over crushed ice for 20 min and stored at −40 °C. Transcription reactions were performed in Tris-HCl buffer (40 mM, pH 7.9) containing 250 nM annealed templates, 10 mM $MgCl_2$, 10 mM NaCl, 10 mM dithiothreitol (DTT), 2 mM spermidine, 1 U μL^{-1} RNase inhibitor (RiboLock), 1 mM GTP, 1 mM CTP, 1 mM UTP and/or 1 mM modified UTP **6**, 20 μM ATP, 5 μCi α-^{32}P ATP, and 3 U μL^{-1} T7 RNA polymerase in a total volume of 20 μL. After 3.5 h at 37 °C, reactions were quenched by adding loading buffer (20 μL; 7 M urea in 10 mM Tris-HCl, 100 mM EDTA, 0.05 % bromophenol blue, pH 8). The samples were heated at 75 °C for 3 min and cooled on an ice bath. The samples (4 μL) were loaded on an analytical denaturing polyacrylamide gel (18 %) containing 7 M urea and run at a constant power (11 W) for nearly 4 h. The gel was exposed to X-ray film (1–2 h), and the exposed film was developed, fixed, and dried. The bands corresponding to full-length transcripts were then quantified by using software (GeneTools from Syngene) to determine the transcription yield. The percentage incorporation of modified ribonucleoside triphosphate **6** has been reported with respect to transcription efficiency in the presence of natural NTPs. All reactions were performed in duplicate, and the errors in yields were found to be ≤4 %.

Large-scale transcription reactions: Large-scale transcription reactions with template **D1** were performed in a 250 μL reaction volume under similar conditions to those described above in order to isolate oligoribonucleotides **7** and **8** for further characterization and fluorescence studies. The reaction contained 2 mM GTP, CTP, ATP, and UTP or modified UTP **6**, 20 mM $MgCl_2$, 0.4 U μL^{-1} RNase inhibitor (RiboLock), 300 nM annealed template, and 800 U T7 RNA polymerase. After the reaction had been incubated for 12 h at 37 °C, the precipitated pyrophosphate was removed by centrifugation. The reaction volume was reduced to approximately one third by Speed Vac, and loading buffer (50 μL) was added. The solution was heated at 75 °C for 3 min and cooled on an ice bath. The sample was loaded onto a preparative 20 % denaturing polyacrylamide gel and was run at a constant power (25 W) for nearly 4.5 h. The gel was UV shadowed, and the appropriate band was excized, extracted with 0.3 M sodium acetate, and desalted by using a Sep-Pak classic C18 cartridge. Typical yields of transcripts were 14–15 nmol. Control transcript **7**: $\varepsilon_{260} = 9.10 \times 10^4\,M^{-1}\,cm^{-1}$; modified transcript **8**: $\varepsilon_{260} = 9.86 \times 10^4\,M^{-1}\,cm^{-1}$.

Enzymatic digestion of transcript 8: Modified oligoribonucleotide **8** from a large-scale transcription reaction (nearly 4 nmol) was digested with snake-venom phosphodiesterase I (0.01 U), calf-intestine alkaline phosphatase (1 U μL^{-1}), and RNase A (0.25 μg) in a total volume of 100 μL in 50 mM Tris-HCl buffer (pH 8.5, 40 mM $MgCl_2$, 0.1 mM EDTA) for approximately 12 h at 37 °C. After this period, RNase T1 (0.2 U μL^{-1}) was added, and the sample was incubated for another 4 h at 37 °C. The ribonucleoside mixture obtained was analyzed by reversed-phase analytical HPLC with a Phenomenex-Luna C18 column (250×4.6 mm, 5 μm) at λ = 260 and 320 nm. Conditions: mobile phase A: 50 mM triethylammonium acetate buffer (pH 7.5); mobile phase B: acetonitrile; flow rate: 1 mL min^{-1}; gradient: 0–10 % B over 20 min and 10–100 % B over 10 min.

Acknowledgements

We thank Prof. Sanjeev Galande for providing the facility to perform radiolabeling experiments. S.G.S. is grateful to the Department of Science and Technology, India for the financial support. A.A.T. is thankful to the Council of Scientific and Industrial Research, India for a graduate research fellowship.

[1] M. J. Rist, J. P. Marino, *Curr. Org. Chem.* **2002**, *6*, 775–793.
[2] A. Okamoto, Y. Saito, I. Saito, *J. Photochem. Photobiol. C* **2005**, *6*, 108–122.
[3] G. M. Wilson, *Rev. Fluoresc.* **2005**, *2005*, 223–243.
[4] U. Asseline, *Curr. Org. Chem.* **2006**, *10*, 491–518.
[5] X. Shi, D. Herschlag, *Methods Enzymol.* **2009**, *469*, 287–302.
[6] R. W. Sinkeldam, N. J. Greco, Y. Tor, *Chem. Rev.* **2010**, *110*, 2579–2619.
[7] S. G. Srivatsan, A. A. Sawant, *Pure Appl. Chem.* **2011**, *83*, 213–232.
[8] a) M. Daniels, W. Hauswirth, *Science* **1971**, *171*, 675–677; b) J. M. L. Pecourt, J. Peon, B. Kohler, *J. Am. Chem. Soc.* **2000**, *122*, 9348–9349; c) E. Nir, K. Kleinermanns, L. Grace, M. S. de Vries, *J. Phys. Chem. A* **2001**, *105*, 5106–5110.
[9] J. N. Wilson, E. T. Kool, *Org. Biomol. Chem.* **2006**, *4*, 4265–4274.
[10] R. T. Ranasinghe, T. Brown, *Chem. Commun.* **2005**, 5487–5502.
[11] M. E. Hawkins in *Topics in Fluorescence Spectroscopy, Vol. 7: DNA Technology* (Ed.: J. R. Lakowicz), Kluwer Academic/Plenum, New York, **2003**, pp. 151–175.
[12] Selected examples of DNA modification: a) L. H. Thoresen, G. S. Jiao, W. C. Haaland, M. L. Metzker, K. Burgess, *Chem. Eur. J.* **2003**, *9*, 4603–4610; b) R. S. Coleman, M. A. Mortensen, *Tetrahedron Lett.* **2003**, *44*, 1215–1219; c) S. T. Gaballah, J. D. Vaught, B. E. Eaton, T. L. Netzel, *J. Phys. Chem. B* **2005**, *109*, 5927–5934; d) N. J. Greco, Y. Tor, *J. Am. Chem. Soc.* **2005**, *127*, 10784–10785; e) F. Seela, E. Schweinberger, K. Y. Xu, V. R. Sirivolu, H. Rosemeyer, E. M. Becker, *Tetrahedron* **2007**, *63*, 3471–3482; f) M. Mizuta, K. Seio, K. Miyata, M. Sekine, *J. Org. Chem.* **2007**, *72*, 5046–5055; g) K. Tainaka, K. Tanaka, S. Ikeda, K. I. Nishiza, T. Unzai, Y. Fujiwara, I. Saito, A. Okamoto, *J. Am. Chem. Soc.* **2007**, *129*, 4776–4784; h) P. Sandin,

K. Borjesson, H. Li, J. Martensson, T. Brown, L. M. Wilhelmsson, B. Albinsson, *Nucleic Acids Res.* **2008**, *36*, 157–167; i) N. A. Grigorenko, C. J. Leumann, *Chem. Commun.* **2008**, 5417–5419; j) Y. N. Teo, J. N. Wilson, E. T. Kool, *J. Am. Chem. Soc.* **2009**, *131*, 3923–3933; k) A. Dumas, N. W. Luedtke, *J. Am. Chem. Soc.* **2010**, *132*, 18004–18007; l) W. Hirose, K. Sato, A. Matsuda, *Angew. Chem.* **2010**, *122*, 8570–8572; *Angew. Chem. Int. Ed.* **2010**, *49*, 8392–8394; m) A. Omumi, D. G. Beach, M. Baker, W. Gabryelski, R. A. Manderville, *J. Am. Chem. Soc.* **2011**, *133*, 42–50; n) T. Ehrenschwender, H. A. Wagenknecht, *J. Org. Chem.* **2011**, *76*, 2301–2304; o) A. Nadler, J. Strohmeier, U. Diederichsen, *Angew. Chem.* **2011**, *123*, 5504–5508; *Angew. Chem. Int. Ed.* **2011**, *50*, 5392–5396.

[13] Selected examples of RNA modification: a) A. Arzumanov, F. Godde, S. Moreau, J. J. Toulme, A. Weeds, M. J. Gait, *Helv. Chim. Acta* **2000**, *83*, 1424–1436; b) S. Shandrick, Q. Zhao, Q. Han, B. K. Ayida, M. Takahashi, G. C. Winters, K. B. Simonsen, D. Vourloumis, T. Hermann, *Angew. Chem.* **2004**, *116*, 3239–3244; *Angew. Chem. Int. Ed.* **2004**, *43*, 3177–3182; c) M. Kaul, C. M. Barbieri, D. S. Plich, *J. Am. Chem. Soc.* **2006**, *128*, 1261–1271; d) K. Lang, R. Rieder, R. Micura, *Nucleic Acids Res.* **2007**, *35*, 5370–5378; e) C. Zhao, J. P. Marino, *Tetrahedron* **2007**, *63*, 3575–3584; f) S. G. Srivatsan, Y. Tor, *J. Am. Chem. Soc.* **2007**, *129*, 2044–2053; g) B. Heppell, D. A. Lafontaine, *Biochemistry* **2008**, *47*, 1490–1499; h) C. M. Zhang, C. Liu, T. Christian, H. Gamper, J. Rozenski, D. Pan, J. B. Randolph, E. Wickstrom, B. S. Cooperman, Y. M. Hou, *RNA* **2008**, *14*, 2245–2253; i) S. Roday, M. B. Sturm, D. Blakaj, V. L. Schramm, *J. Biochem. Biophys. Methods* **2008**, *70*, 945–953; j) H. S. Jeong, S. Kang, J. Y. Lee, B. H. Kim, *Org. Biomol. Chem.* **2009**, *7*, 921–925; k) H. Peacock, O. Maydanovych, P. A. Beal, *Org. Lett.* **2010**, *12*, 1044–1047; l) U. Förster, K. Lommel, D. Sauter, C. Grünewald, J. W. Engels, J. Wachtveitl, *ChemBioChem* **2010**, *11*, 664–672; m) Y. Hikida, M. Kimoto, S. Yokoyama, I. Hirao, *Nat. Protoc.* **2010**, *5*, 1312–1323.

[14] a) T. Xia, *Curr. Opin. Chem. Biol.* **2008**, *12*, 604–611; b) K. B. Hall, *Methods Enzymol.* **2009**, *469*, 269–285.

[15] a) D. C. Ward, E. Reich, L. Stryer, *J. Biol. Chem.* **1969**, *244*, 1228–1237; b) M. Kawai, M. J. Lee, K. O. Evans, T. M. Nordlund, *J. Fluoresc.* **2001**, *11*, 23–32; c) E. L. Rachofsky, R. Osman, J. B. A. Ross, *Biochemistry* **2001**, *40*, 946–956.

[16] Depending on the neighboring bases, a reduction in quantum yield of up to 100 fold has been observed. See reference [15a].

[17] The majority of base-modified fluorescent pyrimidine analogues are deoxyribonucleosides. See reference [6].

[18] a) D. A. Berry, K. Y. Jung, D. S. Wise, A. D. Sercel, W. H. Pearson, H. Mackie, J. B. Randolph, R. L. Somers, *Tetrahedron Lett.* **2004**, *45*, 2457–2461; b) R. A. Tinsley, N. J. Walter, *RNA* **2006**, *12*, 522–529; c) A. S. Wahba, A. Esmaeili, M. J. Damha, R. H. E. Hudson, *Nucleic Acids Res.* **2010**, *38*, 1048–1056.

[19] a) S. G. Srivatsan, N. J. Greco, Y. Tor, *Angew. Chem.* **2008**, *120*, 6763–6767; *Angew. Chem. Int. Ed.* **2008**, *47*, 6661–6665; b) Y. Xie, A. V. Dix, Y. Tor, *J. Am. Chem. Soc.* **2009**, *131*, 17605–17614; c) Y. Xie, T. Maxson, Y. Tor, *J. Am. Chem. Soc.* **2010**, *132*, 11896–11897.

[20] Although tryptophan shows useful fluorescence properties, the interpretation of protein fluorescence becomes complicated because proteins often contain multiple fluorescent amino acids. J. R. Lakowicz, *Principles of Fluorescence Spectroscopy*, 3rd ed., Springer, New York, **2006**.

[21] Several modified pyrimidines containing a conjugated aromatic residue at position 5, if incorporated into oligonucleotides, have marginal impact on the secondary structure. However, the conformation around the rotatable aryl–aryl bond, which has a direct effect on the conjugation and, hence, the electronic properties of the extended nucleobase, has been shown to be sensitive to molecular crowding effects. R. W. Sinkeldam, A. J. Wheat, H. Boyaci, Y. Tor, *ChemPhysChem* **2011**, *12*, 567–570.

[22] M. G. Pawar, S. G. Srivatsan, *Org. Lett.* **2011**, *13*, 1114–1117.

[23] For the photophysical properties of ribonucleosides **3** and **4**, see Figure S1, Figure S2, and Table S1 in the Supporting Information.

[24] C. Reichardt, *Chem. Rev.* **1994**, *94*, 2319–2358.

[25] See the Supporting Information for details.

[26] J. Ludwig, *Acta. Biochim. Biophys. Acad. Sci. Hung.* **1981**, *16*, 131–133.

[27] F. Wachowius, C. Höbartner, *ChemBioChem* **2010**, *11*, 469–480.

[28] Enzymatic ligation has been used to synthesize labeled RNAs. a) C. Höbartner, R. Rieder, C. Kreutz, B. Puffer, K. Lang, A. Polonskaia, A. Serganov, R. Micura, *J. Am. Chem. Soc.* **2005**, *127*, 12035–12045; b) R. Rieder, K. Lang, D. Graber, R. Micura, *ChemBioChem* **2007**, *8*, 896–902.

[29] a) F. Huang, G. Wang, T. Coleman, N. Li, *RNA* **2003**, *9*, 1562–1570; b) R. Fiammengo, K. Musilek, A. Jaschke, *J. Am. Chem. Soc.* **2005**, *127*, 9271–9276; c) M. Kimoto, T. Mitsui, Y. Harada, A. Sato, S. Yokoyama, I. Hirao, *Nucleic Acids Res.* **2007**, *35*, 5360–5369; d) S. G. Srivatsan, Y. Tor, *Chem. Asian J.* **2009**, *4*, 419–427; e) G. Stengel, M. Urban, B. W. Purse, R. D. Kuchta, *Anal. Chem.* **2010**, *82*, 1082–1089.

[30] In vitro transcription reactions are known to produce trace amounts of $N+1$ and $N+2$ products. J. F. Milligan, O. C. Uhlenbeck, *Methods Enzymol.* **1989**, *180*, 51–62.

[31] Template sequences that result in a modification near the promoter region are known to affect the transcription efficiencies. J. F. Milligan, D. R. Groebe, G. W. Witherell, O. C. Uhlenbeck, *Nucleic Acids Res.* **1987**, *15*, 8783–8798. See also reference [29d].

[32] a) M. Torimura, S. Kurata, K. Yamada, T. Yokomaku, Y. Kamagata, T. Kanagawa, R. Kurane, *Anal. Sci.* **2001**, *17*, 155–160; b) J. M. Jean, K. B. Hall, *Proc. Natl. Acad. Sci. USA* **2001**, *98*, 37–41.

[33] Photoinduced electron transfer between the fluorophore and adjacent bases promotes nonradiative dissipation of excited-state energy. a) S. Doose, H. Neuweiler, M. Sauer, *ChemPhysChem* **2009**, *10*, 1389–1398; b) S. O. Kelley, J. K. Barton, *Science* **1999**, *283*, 375–381. See also reference [32a].

[34] a) T. M. Nordlund, S. Andersson, L. Nilsson, R. Rigler, A. Gräslund, L. W. McLaughlin, *Biochemistry* **1989**, *28*, 9095–9103; b) C. R. Guest, R. A. Hochstrasser, L. C. Sowers, D. P. Millar, *Biochemistry* **1991**, *30*, 3271–3279.

[35] Steady-state Stern–Volmer titrations with nucleotide monophosphates reveal marginal fluorescence quenching due to collisional interaction (Figure S7 in the Supporting Information).

[36] a) M. E. Hawkins, F. M. Balis, *Nucleic Acids Res.* **2004**, *32*, e62; b) Y. J. Seo, S. Bhuniya, S. Tapadar, J. W. Yi, B. H. Kim, *Bull. Korean Chem. Soc.* **2007**, *28*, 1923–1924; c) S. Ikeda, T. Kubota, M. Yuki, H. Yanagisawa, S. Tsuruma, A. Okamoto, *Org. Biomol. Chem.* **2010**, *8*, 546–551.

[37] a) T. Lindahl, *Nature* **1993**, *362*, 709–715; b) C. D. Mol, S. S. Parikh, C. D. Putnam, T. P. Lo, J. A. Tainer, *Annu. Rev. Biophys. Biomol. Struct.* **1999**, *28*, 101–128.

[38] a) L. A. Loeb, B. D. Preston, *Annu. Rev. Genet.* **1986**, *20*, 201–230; b) W. Zhou, P. W. Doetsch, *Proc. Natl. Acad. Sci. USA* **1993**, *90*, 6601–6605.

[39] a) H. Ide, K. Akamatsu, Y. Kimura, K. Michiue, K. Makino, A. Asaeda, Y. Takamori, K. Kubo, *Biochemistry* **1993**, *32*, 8276–8283; b) J. Lhomme, J. F. Constant, M. Demeunynck, *Biopolymers* **1999**, *52*, 65–83; c) H. Atamna, I. Cheung, B. N. Ames, *Proc. Natl. Acad. Sci. USA* **2000**, *97*, 686–691.

[40] a) E. L. Rachofsky, E. Seibert, J. T. Stivers, R. Osman, J. B. A. Ross, *Biochemistry* **2001**, *40*, 957–967; b) T. Hirose, T. Ohtani, H. Muramatsu, A. Tanaka, *Photochem. Photobiol.* **2002**, *76*, 123–126; c) K. Sato, M. M. Greenberg, *J. Am. Chem. Soc.* **2005**, *127*, 2806–2807; d) L. Valis, N. Amann, H. A. Wagenknecht, *Org. Biomol. Chem.* **2005**, *3*, 36–38; e) E. Fundador, J. Rusling, *Anal. Bioanal. Chem.* **2007**, *387*, 1883–1890; f) Z. Xu, Y. Sato, S. Nishizawa, N. Teramae, *Chem. Eur. J.* **2009**, *15*, 10375–10378.

Received: April 18, 2011
Revised: July 18, 2011
Published online: September 28, 2011

